

Cube-textured nickel substrates for high-temperature superconductors

E D Specht, A Goyal, D F Lee, F A List, D M Kroeger,
M Paranthaman, R K Williams and D K Christen

Oak Ridge National Laboratory, Oak Ridge, TN 37831-6118, USA

Received 2 February 1998

Abstract. The biaxial textures created in metals by rolling and annealing make them useful substrates for the growth of long lengths of biaxially textured material. The growth of overlayers such as high-temperature superconductors requires flat substrates with a single, sharp texture. A sharp cube texture is produced in high-purity Ni by rolling and annealing. We report the effect of rolling reduction and annealing conditions on the sharpness of the cube texture, the incidence of other orientations, the grain size and the surface topography. A combination of high reduction and high-temperature annealing in a reducing atmosphere leads to > 99% cube texture, with a mosaic of 9.0° about the rolling direction, 6.5° about the transverse direction, and 5.0° about the normal direction.

1. Introduction

Rolling and annealing of fcc metals such as Cu, Au, Al and Ni leads to the $\{100\}\langle 100 \rangle$ or ‘cube’ texture (the notation is defined in figure 1) [1]. This is a particularly useful texture for several reasons: it is a sharp texture, it develops with a large fraction of the sample close to the ideal orientation and all grains in an ideal cube texture have a single orientation. The only other rolling textures for cubic crystal structures which share this last property are $\{100\}\langle 011 \rangle$, $\{110\}\langle 001 \rangle$, and $\{110\}\langle 1\bar{1}0 \rangle$. Consider $\{221\}\langle 221 \rangle$, for example: there are four variants, $(221)[1\bar{2}2]$, $(221)[\bar{1}2\bar{2}]$, $(221)[2\bar{1}2]$, and $(221)[\bar{2}1\bar{2}]$. These variants are symmetry related, so they will occur with equal frequency in a rolling texture. They are distinct orientations, with a 39° rotation required to bring one into alignment with another. A film grown epitaxially on such a substrate will contain numerous large-angle grain boundaries.

Cube-textured Ni has been used as a substrate for high-temperature superconductors (HTSs). Its relatively high melting point and resistance to oxidation permit, with the use of buffer layers [2–4], the epitaxial growth of $\text{YBa}_2\text{Cu}_3\text{O}_x$ [5, 6] and $\text{Tl}_{0.78}\text{Bi}_{0.22}\text{Sr}_{1.6}\text{Ba}_{0.4}\text{Ca}_2\text{Cu}_3\text{O}_9$ [7] films. In this report we discuss the optimization of the Ni substrate. What are the requirements for the substrate? In order for the superconducting overlayer (typically $\sim 1 \mu\text{m}$ thick) to be continuous, the substrate must be smooth. A flat substrate has the added benefit of promoting epitaxy. Because the critical current carried by grain boundaries in HTSs drops rapidly for misorientations of more than about 5° [8], the cube texture must be sharp, so a highly oriented epitaxial overlayer may be grown. Other textures are to be avoided. We have determined the optimum rolling reduction and annealing temperature for such a substrate.

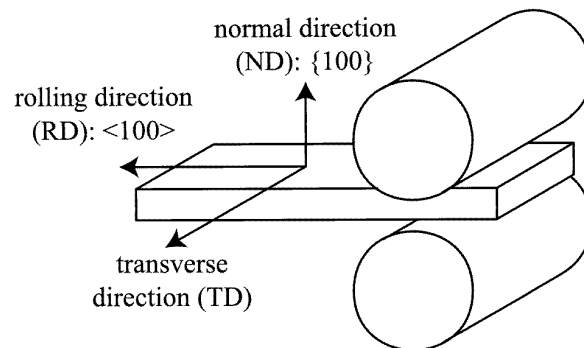


Figure 1. Definition of the notation for the cube rolling texture.

2. Experimental details

High-purity (99.99%), randomly oriented Ni bar is successively rolled to thicknesses of 125–500 μm . Polished work rolls are used in order to produce a smooth Ni surface. We find this more convenient than polishing long lengths of Ni. Samples were annealed for 10 min in a mixture of 0.04 atm H_2 with 0.96 atm Ar. This provides a convenient reducing atmosphere, but the H_2 is not critical to the development of the cube texture. Annealing for 30 min at 1073°C in high vacuum (base pressure of 9×10^{-9} Torr, operating pressure of 1.4×10^{-7} Torr) also produces an optimum texture, equivalent to that of a sample annealed in the H_2 –Ar mixture. A thermocouple spot welded to the sample measured the temperature.

Flatness was measured using atomic force microscopy (AFM) and scanning electron microscopy (SEM). SEM was used to determine grain size.

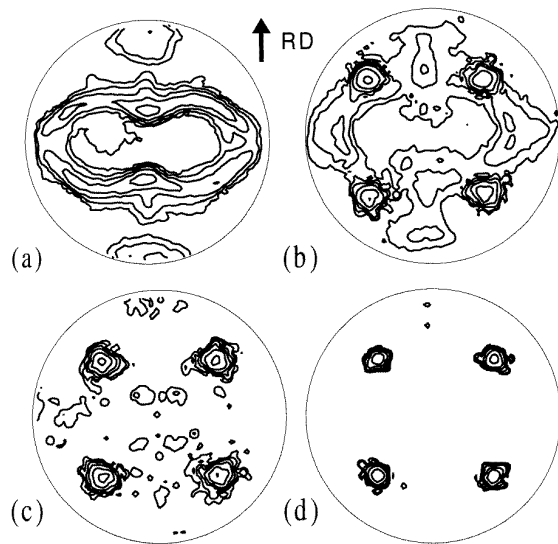


Figure 2. (111) pole figures for 125 μm thick Ni. Contour intervals, selected to highlight weak texture components, are 0.1, 0.3, 1.0, 3.0 and 10.0. Annealing temperature ($^{\circ}\text{C}$): (a) 200; (b) 250; (c) 300; (d) 1372.

The sharpness of the texture was measured using x-ray rocking curves and ϕ scans. A Cu x-ray source was used, with a graphite crystal selecting $K\alpha$ radiation and a four-circle diffractometer orienting the sample. The distribution of tilts was measured by rocking the sample about the RD or TD while observing the out-of-plane (002) reflection (called a rocking curve or ω scan). The distributions of rotations was measured by rotating the sample about the ND while measuring the mixed (202) reflection (called an azimuthal or ϕ scan). Scan widths were determined by least-squares fitting to a Gaussian lineshape; we report the FWHM of the fitted curve. As detailed in the appendix, the width of the (202) reflection overestimates the in-plane misalignment of the sample by a factor of 2. The volume fractions of different texture components were determined by integrating peaks on x-ray pole figures, collected in the Schultz (reflection) geometry [9].

3. Results and discussion

3.1. Texture

Ni retains its rolling texture [10] up to 200 $^{\circ}\text{C}$ (figure 2(a)). For a 300 $^{\circ}\text{C}$ annealing temperature, the primary recrystallization texture [11] is observed, consisting of 94% $\{100\}\langle 100 \rangle$ (cube texture) and 6% $\{221\}\langle 221 \rangle$ (twin texture) (figure 2(c)). The twin texture results from 180 $^{\circ}$ rotation of the cube texture about a $\langle 111 \rangle$ axis. A mixture of rolling and primary recrystallization textures is observed at 250 $^{\circ}\text{C}$ (figure 2(b)). With increasing annealing temperature, the twin texture gradually disappears; for anneals at 1200 $^{\circ}\text{C}$ and above, no twin texture is detected above background (figure 3(b)). No secondary recrystallization was observed, even at 1375 $^{\circ}\text{C}$.

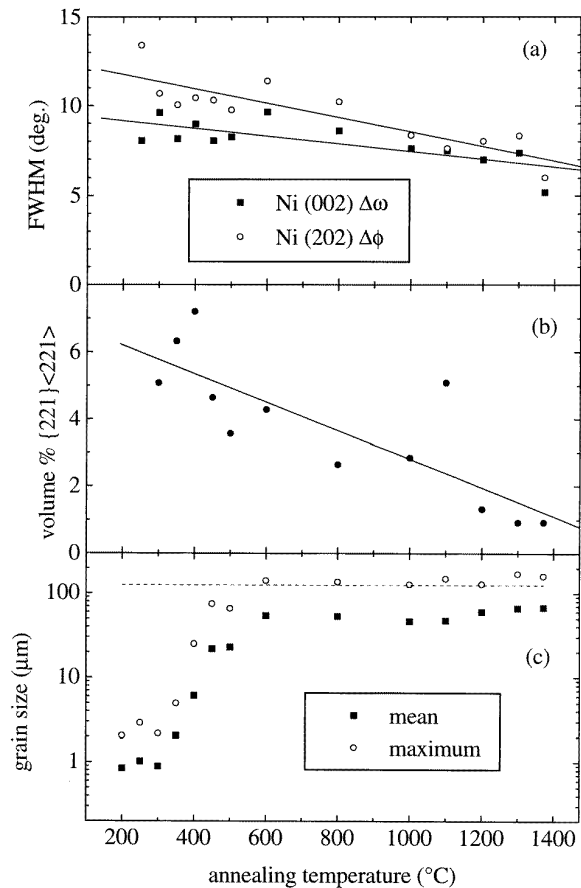


Figure 3. Parameters for samples annealed for 10 min in 4% H_2 : (a) out-of-plane and in-plane alignment, (b) fraction of $\{221\}\langle 221 \rangle$ texture and (c) mean and maximum grain size (broken line indicates sample thickness).

Table 1. Out-of-plane and in-plane mosaic (mean \pm standard deviation) for cube-textured Ni rolled to different thicknesses.

Thickness (μm)	$\Delta\omega$ Ni(002) (deg FWHM)	$\Delta\phi$ Ni(202) (deg FWHM)
125	6.1 ± 0.3	7.3 ± 0.5
250	6.9 ± 0.6	8.75 ± 0.8
500	7.1 ± 1.1	9.9 ± 1.9

The cube texture gradually sharpens with increasing annealing temperature (figure 3(a)). The rocking curve about the TD (out-of-plane alignment) sharpens from 9 $^{\circ}$ to 7 $^{\circ}$ FWHM. The (202) ϕ scan sharpens from 12 $^{\circ}$ to 7 $^{\circ}$, which corresponds to an in-plane alignment sharpening from 6 $^{\circ}$ to 4 $^{\circ}$ (see appendix). Because our primary concern is with rapid processing, we have not systematically investigated the effects of longer anneals. We have verified that the cube texture sharpens with increasing annealing time as well as with increasing annealing temperature. A sample annealed for 10 min at 600 $^{\circ}\text{C}$ had (002) and (202) scan widths of 9.6 $^{\circ}$ and 11.4 $^{\circ}$. Annealing the same sample for a further 1000 min sharpened these widths to 8.0 $^{\circ}$ and 10.4 $^{\circ}$.

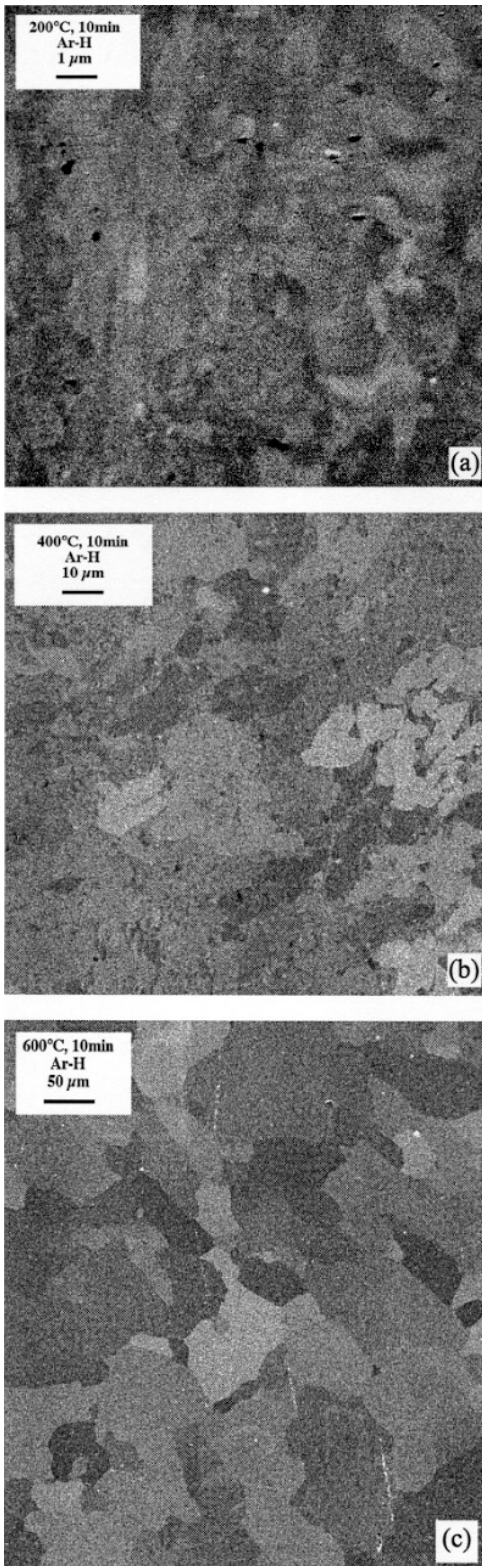


Figure 4. Grain growth, imaged by SEM.

The 125 μm thickness used to measure the effects of different temperatures produces a sharper cube texture than thicker samples (table 1). The breadth of the cube texture increases slowly; the (202) ϕ scan FWHM

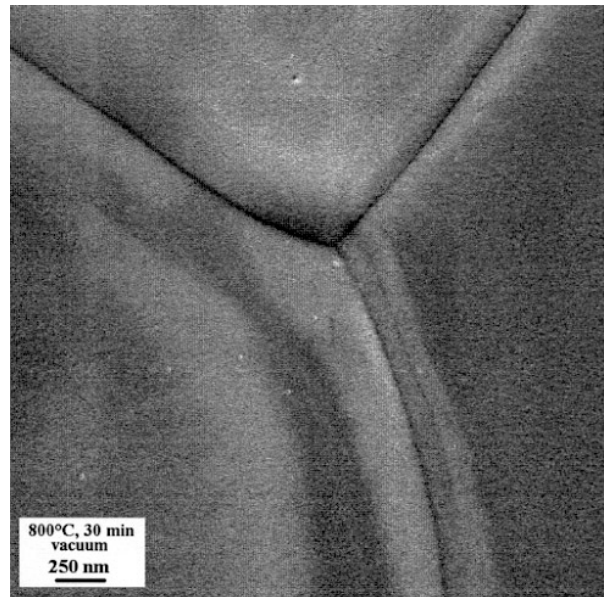


Figure 5. Grain boundary grooving, imaged by SEM.

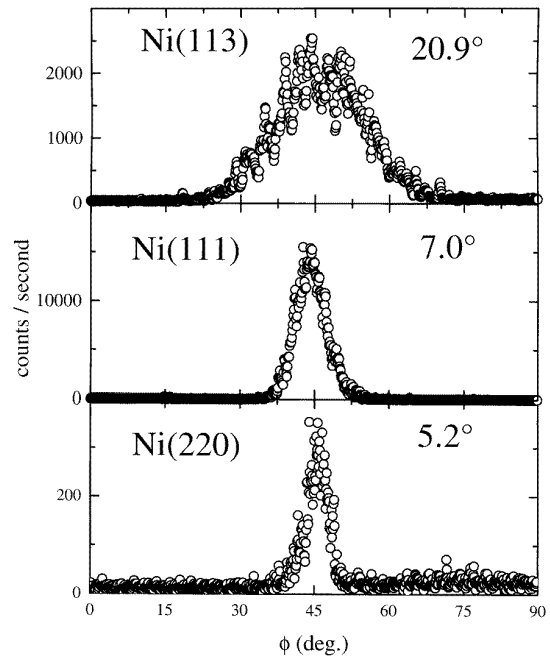


Figure 6. ϕ scans from different reflections for the same cube-textured Ni sample, with FWHM indicated.

increases 47% to 10.7° at 500 μm . Sample-to-sample variability, however, increases dramatically, rising six-fold to a standard deviation of 3.1. This is undesirable, since the current carried by a long wire is determined by its weakest segment. Note that these results were obtained by varying the degree of rolling reduction; further study is needed of the effects of varying the final sample thickness at a constant reduction by changing both the initial and the final sample thickness. Future work will also address the effects of reduction below 125 μm .

3.2. Grain growth

Between 200 and 300 °C, cube-textured grains nucleate with a 1 μm average grain size (figures 3(c) and 4(a)). Between 300 and 600 °C, grain coarsening occurs until the average grain size reaches half the sample thickness (figures 3(c), 4(b) and 4(c)). Secondary recrystallization is signalled by the appearance of a few very large grains. No evidence for this is seen, as the maximum grain size is always about twice the average (figure 3(c)). Note that the texture continues to sharpen well beyond the temperature at which grain growth is complete (figure 3(a) and 3(c)), indicating that the sharpening is due to the rotation of existing grains rather than to selective grain growth.

These results are dramatically different from those of Makita *et al* [11]. Using lower-purity Ni (99.95% versus 99.99%), they find that grain growth occurs at higher temperatures (500–1300 °C), even with much longer annealing times (1–2 h). Further, they find that secondary recrystallization occurs once the grain size reaches its final value; in our samples final grain size is reached at 600 °C but secondary recrystallization does not occur up to 1375 °C.

3.3. Flatness

Average roughness of AFM line scans over a $50 \times 50 \mu\text{m}^2$ area of as-rolled Ni is 10 nm. The surface begins to roughen at 600 °C, on the completion of grain growth. As described by Mullins [12], roughening is caused by grooves which develop at the grain boundaries (figure 5). Further study is needed to quantify this roughness.

4. Conclusions

A wide range of annealing temperatures (300–1375 °C) lead to the development of cube texture in high-purity Ni. Higher temperatures lead to a sharper texture but produce a rougher surface. A thickness of 125 μm leads to an optimum texture.

Acknowledgments

We thank J D Budai for helpful discussions and X Cui for pointing out the variation of ϕ scan width with sample tilt. This research was sponsored by the US Department of Energy, Office of Energy Efficiency and Renewable Energy, Office of Utility Technology–Superconductivity Program and Division of Materials Sciences, under Contract DE-AC05-96OR22464 with Lockheed Martin Energy Research.

Appendix: width of ϕ scans

The distribution of sample tilts about the RD or TD (the out-of-plane alignment) is readily measured by a rocking curve for an out-of-plane peak (a reflection from planes parallel to the surface). Measuring the distribution of rotations about the ND (the in-plane alignment) is more difficult. A ϕ scan for an in-plane peak (a reflection from planes orthogonal to the surface) measures in-plane alignment but presents instrumental difficulties. Measurements made

Table 2. Comparison of observed ϕ scan widths with those calculated using equation (2).

(<i>hkl</i>)	χ	ϕ	W_ϕ (observed)	W_ϕ (calculated)
(113)	65°	45°	20.9	18.0°
($\bar{1}$ 13)	65°	135°	20.5	18.0°
(1 $\bar{1}$ 3)	65°	225°	21.8	18.0°
($\bar{1}$ $\bar{1}$ 3)	65°	315°	21.0	18.0°
(202)	45°	0°	10.8°	10.4°
(022)	45°	90°	8.5°	8.5°
($\bar{2}$ 02)	45°	180°	10.8°	10.4°
(0 $\bar{2}$ 2)	45°	270°	8.3°	8.5°
(111)	35°	45°	7.0°	7.5°
($\bar{1}$ 11)	35°	135°	7.1°	7.5°
(1 $\bar{1}$ 1)	35°	225°	7.2°	7.5°
($\bar{1}$ $\bar{1}$ 1)	35°	315°	7.6°	7.5°

in transmission typically require high-energy x-rays and provide low sensitivity to thin films. Measurements made in reflection require the use of small glancing angles.

In this work we follow the common practice of using ϕ scans from mixed peaks (those which are neither in-plane nor out-of-plane) as an measure of in-plane alignment. In this appendix, we present a simple model relating ϕ scan width to in-plane alignment and show that the width can be substantially overestimated.

Both the in-plane and the out-of-plane sample alignments contribute to the width of a ϕ scan for a mixed peak. Consider a scan taken at a tilt $90^\circ - \chi$ from the ND and an azimuth ϕ from the RD, and let W_{ND} , W_{RD} and W_{TD} be the widths of the distributions of tilts and rotations about the three principal directions. As derived by Srikant *et al* [13] the ϕ scan width will be the convolution of three distributions with widths

$$\Delta\phi_{RD} = W_{RD} |\tan \chi \cos \phi|$$

$$\Delta\phi_{TD} = W_{TD} |\tan \chi \sin \phi| \quad \Delta\phi_{ND} = W_{ND}. \quad (1)$$

We have expanded Srikant *et al*'s results to first order in the widths and converted rocking curve widths to ϕ scan widths. Assuming Gaussian distributions, the total width will be

$$W_\phi = [(W_{RD} \tan \chi \cos \phi)^2 + (W_{TD} \tan \chi \sin \phi)^2 + W_{ND}^2]^{1/2}. \quad (2)$$

For an isotropic sample, $W_{ND} = W_{RD} = W_{TD} \equiv W$ and $W_\phi = W / \cos^2 \chi$. In this case, a ϕ scan for a (202) reflection will overestimate the in-plane width by a factor of 2.

We compare the predictions of equation (2) with ϕ scan widths for cube-textured Ni. Rocking curves of the Ni(002) at $\phi = 0^\circ$ and 90° show that $W_{RD} = 9.1^\circ$ and $W_{TD} = 6.9^\circ$. The in-plane alignment was measured using ϕ scans of the eight {200} and {220} reflections, which are centred at $\chi = 0^\circ$. At this angle, the sample is edge on in the beam and no diffraction is observed, so the scans were taken at $\chi = 5^\circ$, the tilt at which diffracted intensity is maximum. The mean \pm standard deviation for the eight scans is $W_{ND} = 5.0 \pm 0.75$. Because of the large grain size of the samples, all scans are noisy, consisting of sharp peaks from a few hundred grains. The in-plane scans were taken 5° off centre in χ , so fewer grains diffracted, and the

noise-induced variation in peak width was larger. Typical ϕ scans are shown in figure 6. In table 2, measured widths are compared with those calculated using equation (2). Good quantitative agreement is observed in all cases.

For Ni substrates and for typical buffer layers, the (111) reflection provides the best measure of in-plane mosaic W_{ND} . Accuracy can be improved by measuring W_{RD} and W_{TD} from (002) rocking curves and using equation (2) to deduce W_{ND} from W_ϕ . As the reader may have noticed, we reached this conclusion only after collecting the (202) ϕ scans presented here. Do as we say, not as we do. Because of their highly anisotropic growth rates, HTS films grown on smooth substrates typically have much smaller W_{RD} and W_{TD} than the substrates. As a result, $W_\phi \approx W_{ND}$, and peak selection becomes less critical.

References

- [1] Barrett C S and Massalski T B 1966 *Structure of Metals* (New York: McGraw-Hill)
- [2] Christen D K *et al* 1996 *Czech. J. Phys.* **46** 1531
- [3] Paranthaman M *et al* 1997 *Physica C* **275** 266
- [4] He Q *et al* 1997 *Physica C* **275** 155
- [5] Goyal A *et al* 1996 *Appl. Phys. Lett.* **69** 1795
- [6] Norton D P *et al* 1996 *Science* **274** 755
- [7] Ren Z F *et al* 1998 *J. Supercond.* **11** 159
- [8] Dimos D, Chaudhari P, Mannhart J and LeGoues F K 1988 *Phys. Rev. Lett.* **61** 219
- [9] Schultz L G 1949 *J. Appl. Phys.* **20** 1030
- [10] Ray R K 1995 *Acta Metall.* **43** 3861
- [11] Makita H, Hanada S and Izumi O 1988 *Acta Metall.* **36** 403
- [12] Mullins W W 1957 *J. Appl. Phys.* **28** 333
- [13] Srikant V, Speck J S and Clarke D R 1997 *J. Appl. Phys.* **82** 4286